

Characterizing Cocoa Butter Seed Crystals by the Oil-in-Water Emulsion Crystallization Method

Scott A. Hindle^a, Malcolm J.W. Povey^{a,*}, and Kevin W. Smith^b

^aProcter Department of Food Science, University of Leeds, Leeds, LS2 9JT, United Kingdom, and ^bUnilever Research, Colworth Laboratory, Bedford, United Kingdom

ABSTRACT: Unambiguous quantitative evidence for the catalytic action of seed crystals in cocoa butter is presented. We used an ultrasound velocity technique to determine the isothermal growth of solid fat content in cocoa butter oil-in-water emulsions, in which the probability of finding a seed crystal in any one droplet was around 0.37 at 14.2°C. The upper limit for the size of seed crystals in West African cocoa butter was around 0.09 μm , the Gibbs free energy for nucleation was 0.11 mJ m^{-2} , and the concentration of seed crystals was in the range of 10^{16} to 10^{17} m^{-3} . X-ray diffraction measurements showed that emulsified cocoa butter crystallizes in the α polymorph and does not appear to transform to the β' form within the first 25 min of crystallization. Primary nucleation events in cocoa butter emulsions are accounted for by seed crystals. Collision-mediated nucleation, a secondary nucleation mechanism, in which solid droplets (containing seed crystals) catalyze nucleation in liquid droplets, is shown to account for subsequent crystallization. This secondary nucleation mechanism is enhanced by stirring.

Paper no. J10250 in *JAOCS* 79, 993–1002 (October 2002).

KEY WORDS: Cocoa butter crystallization, nucleation, nucleation kinetics, seed crystal, sodium caseinate, Tween 20, ultrasound velocity

Cocoa butter (CB) is one of the most expensive ingredients in chocolate, amounting to 25 to 36% of the finished product and being responsible for the mouthfeel, gloss, and texture of the product. CB is highly polymorphic (1,2), and its polymorphic form is controlled very carefully during the tempering process. Consequently, understanding the crystallization of CB is important. CB crystallization has been extensively investigated in recent years, (3–6). One of the key findings suggested that high-melting seed crystals dominate nucleation (3). Seed crystals are complex and partially understood structures of fats, phospholipids, glycolipids, and possibly water. Dimick (6) proposed that at the initial stages of crystallization the polar lipids take the form of an inverse hexagonal mesophase (H_{II}) with trace amounts of water acting as the core, and then successively lower m.p. TG load onto the polar seed core.

The first stage in the process of solidification is nucleation. Turnbull and others have provided substantial theoretical in-

formation with respect to the kinetics of the nucleation process (7–11). The crystallization kinetics of a bulk fat may be somewhat different from those of the fat dispersed as an emulsion. The emulsified oil generally crystallizes at a temperature much lower than that of the bulk oil (12,13). For example, on cooling, the oil in submicrometer *n*-hexadecane droplets crystallizes 13 to 15°C lower than the thermodynamic m.p., whereas oil in bulk *n*-hexadecane crystallizes after only a few degrees of supercooling (14). The crystallization behavior of emulsified oil depends on, among other things, the mean droplet size, the type of emulsifier used, and the nature of droplet–droplet interactions (14). The great advantage of forming emulsions in order to study crystal nucleation is that detailed nucleation kinetics of heterogeneous nucleation in fats can be determined using the methodology of Turnbull (15). In this work we use nondestructive ultrasound to determine solid fat content (SFC), a technique capable of high accuracy and sensitivity (16). The fitting of nucleation models (9,10) to precise plots of experimental solids against time during isothermal crystallization gives the nucleation rate and other important information. For example, the type of nucleation can be determined by which model fits experimental data best. Thus, whether nucleation is homogeneous or heterogeneous can be evaluated, and whether it occurs at the surface or in the bulk volume. In the case of heterogeneous nucleation, the number concentration of catalytic impurities (responsible for catalyzing nucleation) can be determined. Further, if the particle size distribution is known, an approximation for the number of catalytic impurities per emulsion droplet can be determined. More detailed calculations lead to the determination of the Gibbs free energy of the nucleating surface and the sensitivity of the “activity” of catalytic impurities to temperature. The effects of changing particle size and emulsifier, the degree of undercooling, and many more variables can be investigated with regard to the nucleation of a particular sample (16).

Previous work (15) focused on CB oil-in-water emulsions stabilized with Tween 20. Here, results are presented using CB oil-in-water emulsions stabilized with the protein sodium caseinate in addition to those stabilized with Tween 20. Both short- and long-term isothermal crystallization data are presented, which, together with nucleation kinetics, give quantitative evidence of the CB seed crystal nucleation phenomenon. X-ray diffraction is also used to determine the polymorphic state of CB during crystallization.

*To whom correspondence should be addressed.
E-mail: m.j.w.povey@food.leeds.ac.uk

MATERIALS AND METHODS

A complete description of the methodology applied here to investigate CB oil-in-water emulsion crystallization using ultrasound velocity measurements can be found in Hindle *et al.* (15). WACB (West African cocoa butter) was used as the dispersed oil phase. When subjected to cooling and heating at 1°C/h, bulk crystallization started at ~21.3°C, and melting was complete at ~32.0°C. Note that if an oil such as CB is not dispersed, obtaining meaningful velocity measurements is not possible due to excess signal attenuation (this occurs shortly after the formation of the solid phase). In the emulsion, under the same conditions, crystallization started at ~14.0°C. WACB oil-in-water emulsions were prepared, unless stated otherwise, as follows. Subsequent to heating to 110°C for 1 h, a premix consisting of 20.75% vol/vol WACB, 1.00 wt% sodium caseinate, or 0.80% vol/vol Tween 20, and the remainder double-distilled water was homogenized under high pressure (Shields S500, York, England; hole size 2 mm and pressure ~300 bar) at a rate of 5 min per 100 mL of emulsion. Particle size measurements, using a Malvern Mastersizer MS2000, were made to enable nucleation kinetics calculations and to check emulsion stability. In addition to the particle size distribution, d_{32} values were calculated by the Mastersizer. The term d_{32} is the surface area moment mean, being $\Sigma d^3/\Sigma d^2$ where d is the diameter. Emulsions were contained within a UVM1 cell (ultrasound velocity meter; Cygnus Ltd., Dorchester, United Kingdom) of internal size 4 cm diameter and 7 cm height, situated in a temperature-controlled water bath for analysis. Sound velocity measurements were accurate to within 1.0 m s⁻¹, and the precision was better than 0.1 m s⁻¹. Temperature measurement accuracy was ±0.1°C. Solid content in the CB was determined by the sound velocity method to an accuracy of better than 1.0% and a precision of 0.1%. In the case of isothermal crystallization experiments, samples were quickly cooled (20 to 25°C min⁻¹) to 0.1 to 0.2°C above the desired temperature. Thereafter, emulsions were immediately transferred to the UVM1 cell and velocity measurements started. Each experiment was repeated at least three times.

Nucleation rates in emulsified fats can be determined by measuring the volume fraction of solid fat (ϕ) as a function of time (t). One assumes that after the onset of nucleation complete crystallization is effectively instantaneous; hence, the volume crystallization rate is determined by the nucleation rate (9–11). In the case of homogeneous nucleation, catalyzed either in the bulk volume or at the droplet boundary, the isothermal crystallization rate is determined by only one fit parameter, i.e., J , the nucleation rate. Taking into account droplet size distribution, the volume fraction of solid fat is:

$$\phi = 1 - \int_0^{\infty} \phi_d^0 \exp(-kt) \delta d \quad [1]$$

where k is the reaction rate constant and ϕ_d^0 is the differential volume fraction of droplets with sizes between d and $d + \delta d$. Constant k is expressed as a function of J such that $k = Jv_d$ (v_d being the droplet volume) or $k = Ja_d$ (a_d being the droplet area).

In the case of heterogeneous nucleation, catalytic impurities are present to catalyze the nucleation process; thus, the process cannot be modeled by a single parameter. Now the parameters are J and N_{imp} (the number density of catalytic impurities). If it is assumed that the catalytic impurities are distributed randomly, the maximal achievable volume fraction of solid droplets can be related to the number of impurities per volume by:

$$\phi_m = 1 - \exp(-v_d N_{\text{imp}}) \quad [2]$$

where ϕ_m is the volume fraction of solids at the end of the crystallization process (i.e., there is unlikely to be a catalytic impurity in each droplet, hence $\phi_m < 1$).

Walstra and Beresteyn (12) showed that the volume fraction of solids during heterogeneous nucleation as a function of time can be expressed as:

$$\phi = \phi_m \cdot \frac{J_0 v_d t}{1 + J_0 v_d t} \quad [3]$$

where J_0 is the maximum nucleation rate.

Furthermore, the number of catalytic impurities per droplet, n , can be determined by summing the following relationship over all particle sizes:

$$n = \int_0^{\infty} N_{\text{imp}} v_d \quad [4]$$

Finally, the surface Gibbs free energy of the nucleating surface can be determined by taking the gradient of a plot of $\ln J_0$ against $1/(T\Delta T^2)$, with ΔT^2 being the difference between the crystallization temperature and the melting temperature of the α polymorph of the nucleating surface.

X-ray diffraction (XRD) was used to characterize the crystal polymorphs formed in the emulsion droplets during isothermal crystallization. A Philips generator and Philips PW1050 goniometer with X'Pert APD software running on a Compaq Deskpro XE450 PC were used to obtain XRD patterns. WACB oil-in-water emulsions were prepared as described above. CB emulsions with a greater amount of dispersed oil phase were also prepared (the emulsifier concentration was increased accordingly). CB samples were pressed into a sample holder of dimensions *ca.* 10 × 10 × 1 mm, to present a flat surface to a CuK radiation beam of wavelength Å 1.54. The diffraction pattern was obtained between 18 and 26 angle 2 ϕ over a 6-min period.

In recent years our understanding of CB polymorphism has changed. Traditionally, the various polymorphs were defined as Forms I through to VI (1); however, these are now referred to as γ , α , β' (this now being considered a phase range) and β -V and β -VI (2). The methodology of van Malssen *et al.* (2) is used here.

RESULTS AND DISCUSSION

Short-term isothermal crystallization of CB oil-in-water emulsions. Isothermal crystallization experiments were

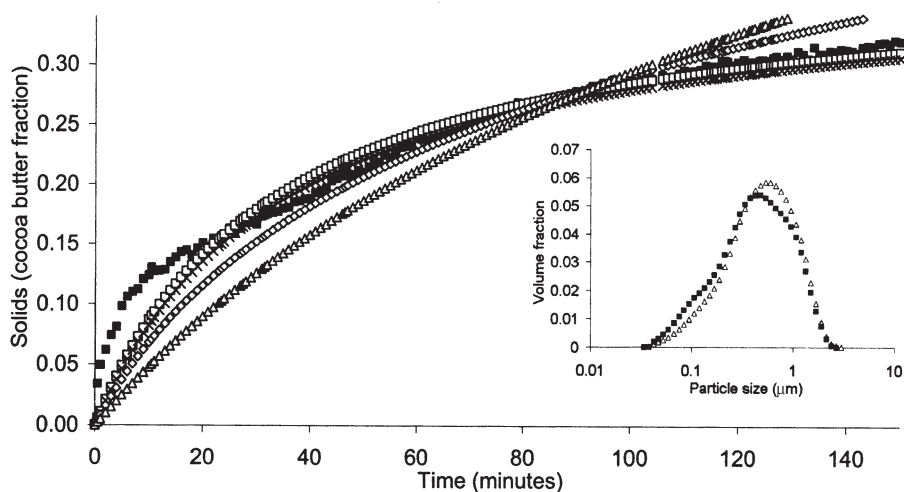


FIG. 1. Plot of solids against time for a 20.75% vol/vol West African cocoa butter (WACB) oil-in-water emulsion (1.00 wt% sodium caseinate) crystallized isothermally at 15.0°C (■ experimental data). The following nucleation models are fitted based on particle size distribution; □ volume heterogeneous, × surface heterogeneous, ◇ volume homogeneous, and △ surface homogeneous. [Insert: Representation of the particle size distribution of two WACB oil-in-water emulsions following emulsion production, △ stabilized with sodium caseinate (1.00 wt%), and ■ with Tween 20 (0.80% vol/vol).]

performed following calibration of the emulsion system, i.e., determination of the liquid and solid velocity equations (for details see Ref. 16). Nucleation models were fitted to plots of experimentally determined solids against time for the isothermal crystallization of our CB emulsions. Figure 1 illustrates the crystallization data of a sodium caseinate-stabilized emulsion at 15.0°C with the accompanying nucleation model fits. All models were calculated using the particle size distribution data obtained *via* the Malvern Mastersizer MS2000, made after preparation of the emulsion (see Fig. 1, insert) and remeasured at the end of the experiment. The d_{32} for these sodium caseinate-stabilized emulsions was $0.296 \pm 0.005 \mu\text{m}$; this low figure and narrow distribution indicate an emulsion of good stability. It is apparent from Figure 1 that the heterogeneous models fit the data more closely than those based on homogeneous nucleation. Furthermore, it appears reasonable to assume that the best fit is obtained for the heterogeneous volume particle size distribution model. This is based on the fact that it more closely represents primary nucleation events. Nevertheless, the most striking feature, and what is most important to observe in Figure 1, is that no single model accurately represents the experimental data over the 150-min period. Turnbull and Cormia (10) and Kloeck (17) successfully used these fits to account for the crystallization in their samples over similar time periods; thus CB oil-in-water emulsions do not strictly adhere to the mechanism of Turnbull and Cormia (10). Figure 1 suggests therefore that at least two nucleation mechanisms account for CB crystallization in oil-in-water emulsions. It is suggested that CB seed crystals act initially and are responsible for primary nucleation events in CB oil-in-water emulsions. The secondary nucleation mecha-

nism, acting subsequently to CB seed crystals, is hypothesized to be droplet collision-mediated nucleation.

The initial phase (0–10 min) of the isothermal crystallization of sodium caseinate stabilized-CB oil-in-water emulsions has been investigated in detail. Figure 2 shows the very accurate fitting of heterogeneous volume particle size distribution nucleation models to isothermal crystallization plots of solids against time for WACB emulsions stabilized with sodium caseinate. Nucleation rates were found to be between 9.17×10^{15} and $3.23 \times 10^{16} \text{ m}^{-3} \text{ s}^{-1}$ and the seed crystal concentration was found to be in the range 2.74×10^{16} to $2.33 \times 10^{17} \text{ m}^{-3}$ (Note: the lower values refer to isothermal crystallization at 15.8°C and the higher values to 14.2°C). At a seed crystal concentration of $2.33 \times 10^{17} \text{ m}^{-3}$ the probability of finding a seed crystal in any one droplet is around 0.37. Additionally, the Gibbs free energy of the nucleating surface in our CB samples was estimated to be 0.11 mJ m^{-2} . A comparison of data obtained from Figure 2, sodium caseinate-stabilized emulsions, with those shown in Hindle *et al.* (15), Tween 20-stabilized emulsions, suggests that conclusions made in Hindle *et al.* (15) pertaining to CB seed crystal activity in primary nucleation hold true here. Hence, we conclude that this primary nucleation phase is dominated by CB seed crystal nucleation, occurring in the bulk volume of the oil droplet and independently of the emulsifier used. Notably, in the case of sodium caseinate-stabilized emulsions, the difference between the crystallization profiles at 15.5 and 15.8°C is small. This suggests that CB seed nuclei are extremely temperature sensitive, as above 15.5°C the rate of solidification is very low. Below this temperature the nucleation increases rapidly.

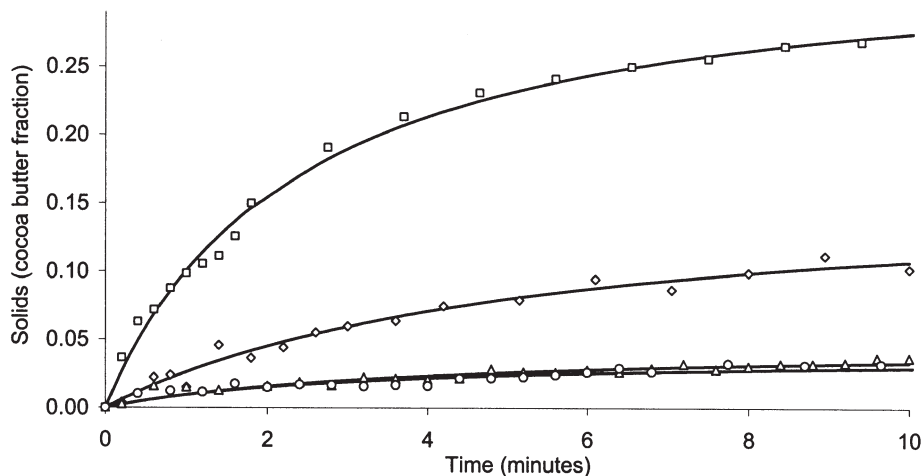


FIG. 2. Plot of solids against time for 20.75% vol/vol WACB oil-in-water emulsions (1.00 wt% sodium caseinate) crystallized at \square 14.2, \diamond 15.0, \triangle 15.5, and \circ 15.8°C. Heterogeneous volume particle size distribution nucleation models are fitted to experimental data (shown as solid lines). For abbreviation see Figure 1.

A plot of solids fraction against particle diameter is shown (Fig. 3) based on the knowledge of the number of crystal nuclei per unit volume in the sodium caseinate-stabilized CB emulsions. This is essentially a representation of the dependence of solid fat content on particle size. Thus, below a certain droplet size the probability of one of these droplets containing a catalytic impurity (i.e., CB seed crystal) able to initiate nucleation is negligibly small. Figure 3 illustrates the temperature sensitivity of CB seed crystals. For example, at a 1- μm oil droplet size the calculated solids fraction at 15.5 and 15.8°C (based on the number of catalytic impurities determined per unit volume, N_{imp} , values of $2.86 \times 10^{16} \text{ m}^{-3}$ and $2.74 \times 10^{16} \text{ m}^{-3}$, respectively) is around 0.02, whereas at 14.2°C ($N_{\text{imp}} = 2.33 \times 10^{17} \text{ m}^{-3}$) this value approaches 0.14.

It can be concluded therefore that at 15.5 and 15.8°C very few active seed nuclei would likely be found in emulsion droplets of less than 1 μm diameter.

Long-term isothermal crystallization of CB oil-in-water emulsions. In previous work (15), using *n*-hexadecane oil-in-water emulsions, the proposed interdroplet secondary nucleation mechanism was demonstrated *via* the use of a membrane barrier to prevent initial collisions between supercooled liquid and solid emulsion droplets. This is likely to occur through breakdown in the stabilizing emulsifier film at the oil-water interface when pairs of droplets collide, facilitating a bridging phenomenon in which the oil in one of the colliding pairs of droplets contacts the solid in the second drop, leading to crystal nucleation (15). Herhold *et al.* (18) suggested

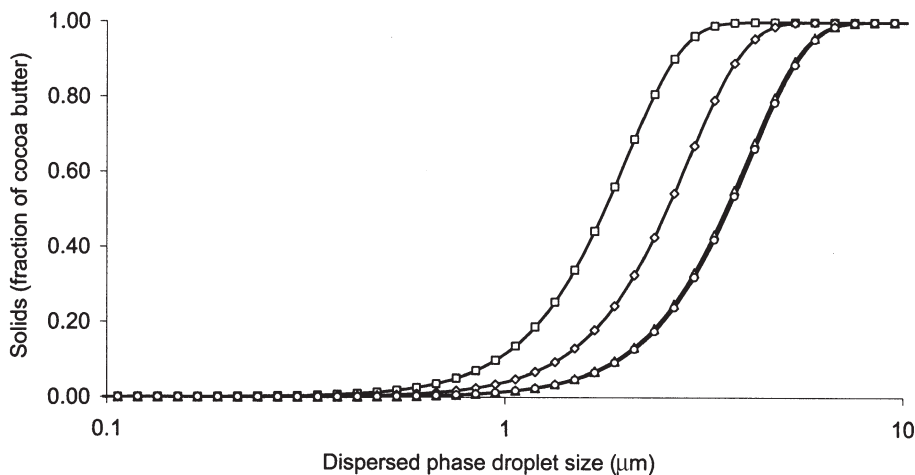


FIG. 3. Plot of solid fat content against cocoa butter emulsion droplet size calculated using the values of catalytic impurities per unit volume determined from the heterogeneous volume nucleation model fits in Figure 2 (\square 14.2, \diamond 15.0, \triangle 15.5, and \circ 15.8°C).

an alternative to the interdroplet nucleation mechanism. Using nearly monodisperse *n*-hexadecane oil-in-water emulsions, they suggested that, upon freezing, droplets expel impurities, possibly due to the presence of the surfactant, and these enter the solution of the liquid *n*-hexadecane droplets and attempt to restore thermodynamic equilibrium. The greater concentration of mobile impurities would thus affect the liquid droplets by reducing their melting temperature, hence producing a decrease in the thermodynamic drive toward solidification (18). Here we do not use this mechanism to explain results. When using a membrane barrier to prevent collisions between solid fat droplets and liquid oil droplets, minimal *n*-hexadecane droplet crystallization occurred (15) despite the fact that the impurities detailed by Herhold *et al.* (18) would be able to cross the barrier. The purpose of these experiments was to look at the long-term crystallization of CB, thus illustrating in greater detail how previous results (15) could be applied to CB oil-in-water emulsions, i.e., that subsequent to primary nucleation catalyzed by CB seed crystals, interdroplet secondary nucleation predominates.

Tween 20-stabilized CB oil-in-water emulsions underwent isothermal crystallization for up to 12 h at the temperatures described above (14.2, 15.0, 15.5, and 15.8°C). As seen in previous experiments at these temperatures, the lower the temperature, the faster the rate at which solidification occurs. To investigate the proposed interdroplet secondary nucleation mechanism (a form of surface nucleation), heterogeneous surface particle size distribution nucleation models were fitted against experimental data. Fits were made using data taken 10 min after the onset of isothermal crystallization since we have already accounted for the primary nucleation mechanism (i.e., CB seed crystals). Figure 4 illustrates the results. The quality of the fits is apparent: The theoretical solids very closely match those experimentally determined. The accuracy

of the heterogeneous surface fits supports the suggestion that a surface mechanism predominates after the initial high activity of the seed crystals. Based on the conclusions derived previously (15), the suggested secondary nucleation mechanism is that of interdroplet nucleation. Particle size distribution measurements taken after 12 h revealed no significant change in d_{32} values. This is perhaps surprising since partial coalescence or flocculation may be expected to occur in these emulsion droplets. However, McClements *et al.* (19) reported no change in particle size distribution following mixing of 50:50 wt% *n*-hexadecane liquid and solid emulsion droplets.

Interestingly, there is no clear moment at which it can be definitively concluded that the secondary nucleation phenomenon begins. Initially, as discussed earlier, the first nucleation phase reflects the very strong effect of the action of CB seed crystals—the scene of the greatest rate of increase in SFC. Beyond the initial 10 min, as shown in Figure 4, there is a greater rate of solidification in the earlier stages (0–100 min) followed by a decline in the rate thereafter. It would seem reasonable to assume that some seed nuclei still initiate nucleation after the first 10 min of crystallization, albeit to a significantly lesser degree. The likelihood is that these less active CB seed crystals would act during this secondary period; thus they could play a role in this phase, although the exact extent is unknown. It also seems reasonable to assume that these remaining seed crystals would not strongly influence bulk CB solidification. Furthermore, it is suggested that the interdroplet nucleation mechanism begins to act as soon as there exists a combination of supercooled liquid and supercooled solid emulsion droplets. Thereafter, as the number of active seed nuclei at the experimental temperature approaches zero, the interdroplet mechanism gains greater significance in relation to the solidification rate. This is also accompanied by the reduced solidification rate seen.

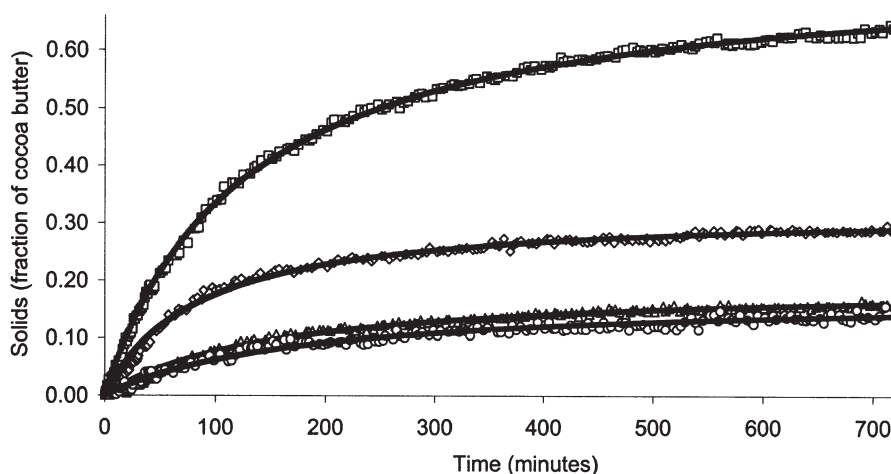


FIG. 4. Plot of solids against time for 20.75% vol/vol WACB oil-in-water emulsions (0.80% vol/vol Tween 20) crystallized at \square 14.2, \diamond 15.0, \triangle 15.5, and \circ 15.8°C. Crystallization post 10 min is shown; thus, time and solids are considered to be zero at this point. Heterogeneous surface nucleation models, based on particle size distribution, are fitted. For abbreviation see Figure 1.

As the number of collisions and the effectiveness of the collisions are directly responsible for the degree of interdroplet secondary nucleation, results are presented regarding these factors. First, the effect of stirring was investigated (i.e., the greater the rate of stirring, the greater the number of collisions), and second, the effect of emulsifier (Tween 20- and sodium caseinate-stabilized emulsions). Thicker, more viscoelastic layers result at droplet surfaces when using milk proteins than small-molecule surfactants (14). For example, caseins appears to protrude from the oil-water-interface to a considerable distance, forming a layer between 10 and 15 nm in thickness, which is substantially larger than the 1 nm layer that forms with Tween 20 (20). Photon correlation spectroscopy can be used to investigate this. McClements *et al.* (21) have already shown that the effective thickness of the adsorbed layer affects the likelihood of droplet-droplet nucleation occurring. Milk proteins therefore reduce the rate of interdroplet heterogeneous nucleation by decreasing the ease with which fat crystals penetrate the interface (14). Consequently, nucleation rates would be anticipated to be lower in sodium caseinate-stabilized emulsions.

The effect of stirring was compared to that against the non-stirred samples already studied. Figure 5 shows the realized plot of solids against time for isothermal crystallization at 15.0°C of standard Tween 20 WACB oil-in-water emulsions post 10 min crystallization. Again, no significant changes in particle size distribution were observed over the 12-h period. Heterogeneous nucleation surface models, based on particle size distribution, were fitted very accurately against experimental data. As the proposed secondary interdroplet mechanism is dependent on the number of collisions (and their effectiveness), the increased use of stirring naturally increases the collision frequency; we estimate collision rates from kinetics later in this paper. If interdroplet nucleation is

the mechanism responsible for the nucleation events occurring, the stirring of emulsions would be anticipated to increase the SFC. Thus, it is proposed that this mechanism accounts for the results seen in Figure 5.

Aside from fitting heterogeneous nucleation models, secondary nucleation kinetics have further applications (see Ref. 14 for details). In interdroplet heterogeneous nucleation, it is assumed that a collision occurs between a single liquid and a single solid droplet, and, as a reactive pair, that crystallization occurs spontaneously. It is also assumed that both the newly formed and the original solid droplet have equal reactivity. Thus, the change in the fraction of liquid oil ($1 - \phi$) remaining after time t is given by:

$$\frac{d(1-\phi)}{dt} = -k_{1s}\phi(1-\phi) \quad [5]$$

where ϕ is the volume fraction of solidified oil and k_{1s} is a second-order rate constant giving the degree of reactivity. Integration of Equation 5 gives:

$$\ln\left[\frac{1-\phi}{\phi}\right] = \ln\left[\frac{1-\phi_o}{\phi_o}\right] - k_{1s}t \quad [6]$$

where ϕ_o is the initial volume fraction of solidified droplets. The rate constant, k_{1s} , can be calculated from the slope of a plot of $\ln[(1-\phi)/\phi]$ against time (19,22), and is dependent upon the collision frequency of the droplets and the effectiveness of the collisions that are able to promote secondary heterogeneous nucleation. The collision frequency for droplets in continuous motion was determined by Smoluchowski (23):

$$n_c = \frac{8k_B T n_0^2}{3\eta} \quad [7]$$

where n_c is the number of collisions per second, k_B is the Boltzmann constant, T is the absolute temperature, n_0 is the

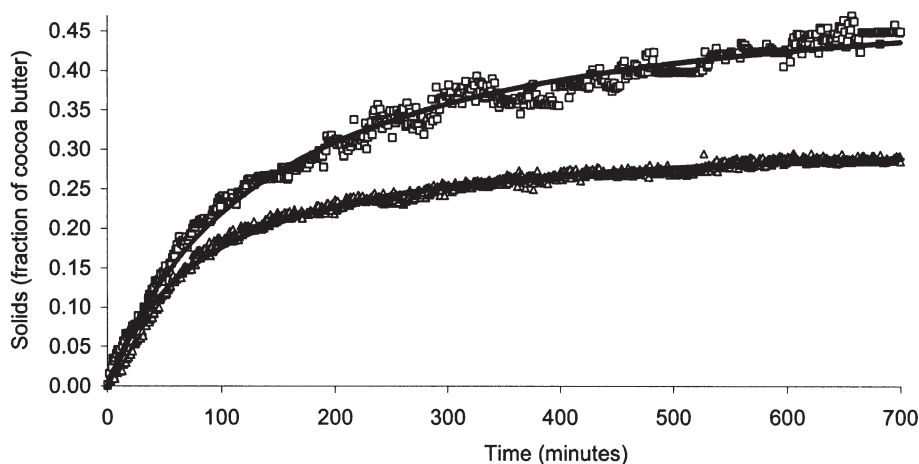


FIG. 5. Plot of solids against time for two 20.75% WACB oil-in-water emulsions (0.80 vol/vol Tween 20) crystallized at 15.0°C. Of the two emulsions, □ was stirred (~250 rpm) and △ was not. Crystallization post 10 min is shown (time and solids are considered to be zero at this point). Heterogeneous surface particle size distribution nucleation models are fitted. For abbreviation see Figure 1.

total number of droplets per unit volume of emulsion, and η is the viscosity of the continuous phase. The fraction of collisions that elicit nucleation can be determined:

$$\frac{1}{W} = \frac{k_{1s}}{n_c/n_0} \quad [8]$$

Finally, the potential energy barrier (E) to interdroplet nucleation can be determined:

$$E = k_B T \ln W \quad [9]$$

This knowledge was applied to the stirred and nonstirred WACB emulsions (Fig. 6). Whereas the heterogeneous surface nucleation models fitted above (based on the research of Turnbull and coworkers) are sufficient to show that this is the type of nucleation occurring (i.e., surface), the specific type of secondary nucleation is not directly identified. For example, surface nucleation is known to be initiated at the droplet boundary if the molecular structures of the dispersed oil phase and the emulsifier are sufficiently similar. The advantage of using the methodology as seen in Figure 6 is that the accurate fitting of a trendline to a plot of $\ln[(1 - \phi)/\phi]$ against time is indicative of the existence of the interdroplet secondary nucleation mechanism. Interestingly, the least accurate area of the plot is during the initial stages; thus, Figure 6 commences at 100 min. Only at around 200 min do the experimental data fit the trendline accurately. This appears to be further evidence to support the suggested CB emulsion crystallization mechanism above. The initial stage is already accounted for (i.e., the role of CB seed crystals). Following this, it appears that more than the interdroplet secondary nucleation mechanism exists, due to the variation in the experimental values and the fitted trendlines. It is therefore likely that CB seed crystals still retain some activity, despite their impact on SFC being reduced. Beyond 200 min, as the trendline and experi-

mental values converge it seems reasonable to assume that interdroplet secondary nucleation becomes more and more prominent.

Quantitative interdroplet secondary nucleation kinetics were determined from Figure 6. By using the equations of the fitted trendlines, the second-order rate constant, k_{1s} , was determined:

$$\text{Stirred emulsion: } k_{1s} = 1.94 \times 10^{-5} \text{ s}^{-1} \quad [11]$$

$$\text{Unstirred emulsion: } k_{1s} = 1.30 \times 10^{-5} \text{ s}^{-1} \quad [12]$$

Furthermore, the potential energy barrier to collision-mediated nucleation was determined:

$$\text{Stirred emulsion: } E = 14.16 k_B T \quad [13]$$

$$\text{Unstirred emulsion: } E = 14.56 k_B T \quad [14]$$

The values obtained are somewhat lower than those determined elsewhere (14; *n*-hexadecane emulsion crystallization), indicating that in this case there is a lower energy barrier to collision-mediated nucleation, and thus this mechanism occurs more readily in these samples.

To clarify the effect of emulsifier type on long-term CB emulsion crystallization, Figure 7 compares two solidification profiles at 15.0°C. Shown is crystallization, post 10 min, of Tween 20- and sodium caseinate-stabilized emulsions. The plots resemble those seen in Figure 5 (the effect of stirring on SFC at 15.0°C). Again, no changes in particle size distribution were observed. Hence, as the volume fraction of SFC is similar in the early stages of the plot, the type of emulsifier appears not to affect the nucleation in this period significantly. Thus, the same conclusions regarding CB seed crystals still apply. As time passes and the supply of active seed crystals is

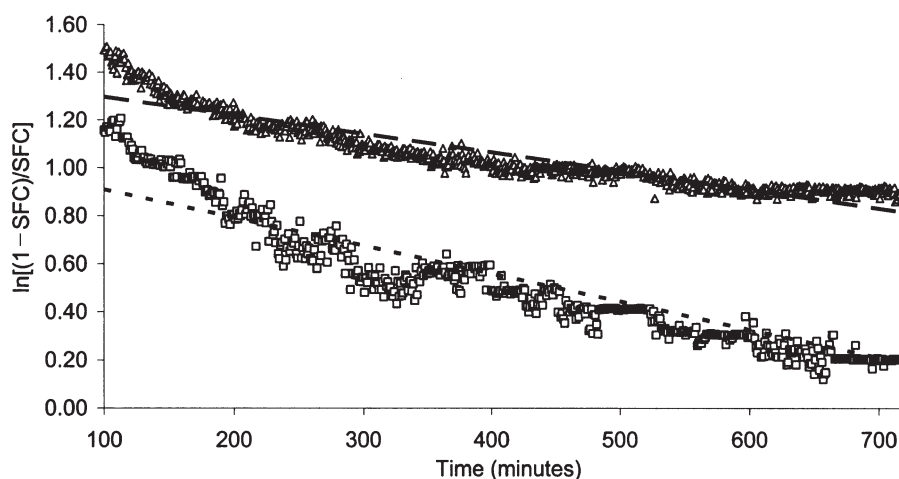


FIG. 6. Plot of $\ln[(1 - \text{SFC})/\text{SFC}]$ against time for two standard WACB oil-in-water emulsions crystallized at 15.0°C as seen in Figure 5. \triangle underwent static crystallization (fitted trendline $y = -0.0008x + 1.38$), whereas \square was subjected to stirring (fitted trendline $y = -0.0012x + 1.03$). SFC, solid fat content; for other abbreviation see Figure 1.

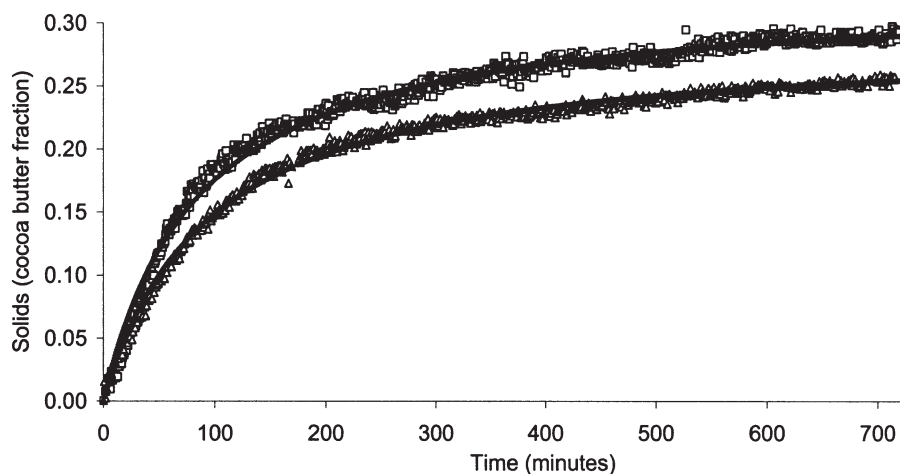


FIG. 7. Plot of isothermal crystallization at 15.0°C (post 10 min) of two 20.75% WACB oil-in-water emulsions. \triangle was prepared with 1.00 wt% sodium caseinate, \square with 0.80% vol/vol Tween 20. Heterogeneous surface nucleation models, based on particle size distribution, are fitted. For abbreviation see Figure 1.

exhausted, the kinetic barrier provided by the emulsifier layer to interdroplet crystallization becomes significant. The sodium caseinate emulsions, having a thicker layer at the droplet surface, have the effect of reducing the likelihood of a fat crystal penetrating the interface and thus decreasing the rate of interdroplet nucleation. At 700 min, the volume fraction of solid CB in the Tween 20-stabilized emulsion is ~ 0.29 , which is greater than that for the sodium caseinate-stabilized emulsion, ~ 0.26 . This behavior is characteristic of interdroplet secondary nucleation as described throughout this work.

XRD. In completing the study of the isothermal crystallization of WACB oil-in-water emulsions, results are presented with regard to polymorphic occurrence. If very rapid polymorphic transformations had occurred, determining the surface Gibbs free energy of the nucleating surface would be more difficult. Although the primary aim was to determine the polymorphic state during the initial phase of nucleation, results in the longer term are also shown, detailing the complex nature of CB. It is noteworthy that good-quality XRD data could be obtained from oil-in-water emulsions. However, the use of oil-in-water emulsions resulted in overall low average intensities.

Figure 8A illustrates the polymorphic state of CB following analysis of a standard WACB emulsion (0.80% vol/vol Tween 20) at 15.0°C. Three experimental runs are shown (each lasting 6 min). Run 1 is the initial analysis following the onset of crystallization. Two clear conclusions may be drawn from this figure. First, there is only one strong response, occurring at $21^\circ 2\theta$. The very strong intensity shown at this point, and the absence of any other peaks suggests that at this stage CB must be in the α polymorph (CB Form II) (1, 2). Second, the intensity of the peak increases with time (i.e., greatest for run 3), signifying an increase in the volume frac-

tion of solid CB (24). This corroborates results seen in ultrasound studies, i.e., that the volume fraction of solid CB increases with time, but is not quantified here using XRD. The X-ray data presented here are particularly interesting as it was feared that no significant response would be initially observable in the 20.75% vol/vol CB emulsions owing to interference from the continuous phase. Since the oil phase only represents about one-fifth of the emulsion, the fraction of the whole sample solidified originally is small. Furthermore, this experiment was repeated with a sodium caseinate-stabilized emulsion (1.00 wt%), giving identical results.

CB emulsions with a greater volume fraction of dispersed phase were produced (41.50% vol/vol and 62.25% vol/vol). These were studied, along with bulk WACB, to evaluate their polymorphism in relation to the standard CB emulsions. All samples initially crystallized into the α polymorph. Figure 8B shows the plot of intensity against diffraction angle for the 41.50% vol/vol CB emulsion. Because a lower energy barrier had to be scaled for nucleation into the α polymorph (compared to that for the β' and β configurations), this outcome was anticipated. Data in Figure 8B show that, when undergoing crystallization at 15.0°C, CB emulsions remain in the α polymorph for at least 25 min (note: each run is of 6 min duration).

Although this work is not a comprehensive study of CB polymorphism, results are presented for solidification beyond the designated initial stage. Figure 8C illustrates the results for analysis of a sodium caseinate-stabilized CB emulsion (20.75% vol/vol) at 15.0°C at the following times after onset of crystallization: 10 min, 2 h, and 4 h. At 10 min the results conclusively suggest that only α is present. Interestingly, at 2 h there is a greater intensity at $\sim 23.0^\circ$. This, along with the strong intensity at 20.9° , is indicative of β' (1,2). As α and β' are both likely to be present, it is impossible (from these data)

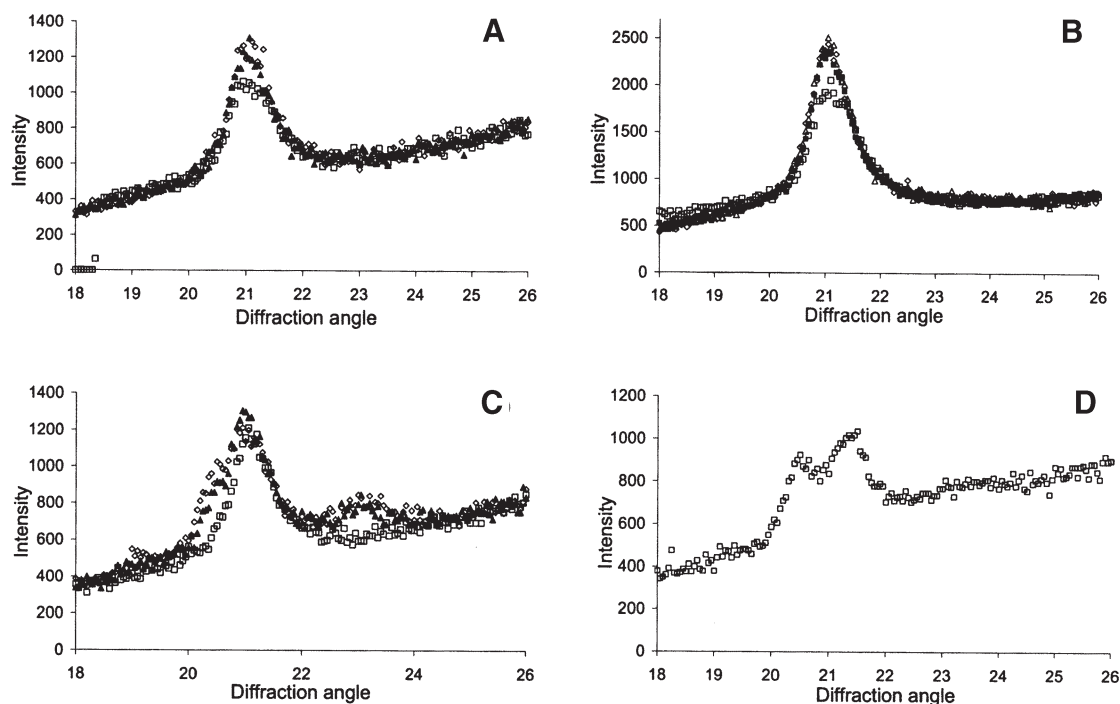


FIG. 8. (A) Plot of intensity against diffraction angle for a standard 20.75% vol/vol WACB oil-in-water emulsion (0.80% vol/vol Tween 20) analyzed immediately at 15.0°C. Each run is of 6 min duration (\square Run 1, \blacktriangle Run 2, \diamond Run 3). (B) Plot of intensity against diffraction angle for a sodium caseinate-stabilized 41.50% vol/vol WACB oil-in-water emulsion analyzed immediately upon reaching 15.0°C (\square Run 1, \blacksquare Run 2, \diamond Run 3, \triangle Run 4). (C) Plot of intensity against diffraction angle for a sodium caseinate-stabilized (1.00 wt%) 20.75% vol/vol oil-in-water emulsion crystallized at 15.0°C. All analyses were performed at 15.0°C (\square 10 min, \blacktriangle after 2 h, \diamond after 4 h). (D) Plot of intensity against diffraction angle for a 20.75% vol/vol WACB oil-in-water emulsion (0.80% Tween 20) allowed to crystallize overnight (\sim 18 h) at 15.0°C. For abbreviation see Figure 1.

to estimate the fractions of the two. At 4 h, however, the slightly greater intensity at the diffraction angle of 23° implies that additional transformation has occurred.

Samples were left overnight (\sim 18 h) in order to determine their polymorphic structures following longer periods of crystallization (Fig. 8D). In the case of the 20.75% vol/vol CB emulsion (to compare with ultrasound data), overnight crystallization resulted in the phase range β' (1,2). Figure 8D is a plot of intensity against diffraction angle. The very strong intensities at 20.4° and 21.4° are indicative of β' (1,2). Overnight crystallization of a 41.50% vol/vol WACB oil-in-water emulsion resulted in observations similar to those deduced from Figure 8D (i.e., the β' phase range). A CB emulsion of dispersed phase 62.25% vol/vol showed a slight increase in intensity at 19.3°, indicating the presence of a small amount of CB β -V (1,2). Nonetheless, this sample was primarily in the phase range β' . Finally, bulk WACB crystallized overnight at 15.0°C was predominantly in the polymorph β -V (data not shown). There was evidence of the existence of some β' crystals, although these would be expected to transform to β -V shortly after. Bulk WACB crystallized overnight at 20.0°C suggested an even greater presence of β -V crystals. Neither of the 20.75% vol/vol WACB oil-in-water emulsions showed any occurrence of crystallization in the oil phase when left overnight at 20.0°C.

Thus, the use of XRD demonstrated that CB oil-in-water

emulsions nucleate in the α polymorph. No evidence for the existence of either β' or β crystals was seen in the first 25 min of isothermal crystallization at 15.0°C. Transformation to β' crystals occurred shortly afterward. At 2 h the presence of β' crystals was apparent. Overnight crystallization revealed that further polymorphic transformation occurred. A much more detailed investigation would have to be performed to determine when transformations occurred (dependent on, for example, temperature) and to what extent. The purpose of this study, however, was to determine the polymorphic state of CB (when emulsified) during the period in which primary nucleation dominated. This was successfully shown to be the α polymorph. These results suggest that the ultrasound technique is insensitive to crystal polymorphic form in CB oil-in-water emulsions since the long-term ultrasound studies show no evidence of the polymorphic changes that XRD demonstrates.

ACKNOWLEDGMENTS

Scott Hindle acknowledges support from the U.K. Biology and Biotechnology Science Research Council and Unilever plc in the form of a CASE award. Acknowledgements are also extended to Dr. Kevin Dilly of Unilever Research (Bedford, United Kingdom) for his assistance with the XRD analysis, and to Dr. William Kloek (Wageningen University, The Netherlands) for help with nucleation kinetics.

REFERENCES

1. Wille, R.L., and E.S. Lutton, Polymorphism of Cocoa Butter, *J. Am. Oil Chem. Soc.* 43:491–496 (1966).
2. van Malssen, K., A. van Langevelde, R. Peschar, and H. Schenk, Phase Behavior and Extended Phase Scheme of Static Cocoa Butter Investigated with Real-Time X-Ray Powder Diffraction, *Ibid.* 76:669–676 (1999).
3. Davis, T.R., and P.S. Dimick, Isothermal and Thermal Characterization of High-Melting Seed Crystals Formed During Cocoa Butter Solidification, *Ibid.* 66:1488–1493 (1989).
4. Dimick, P.S., and D.M. Manning, Thermal and Compositional Properties of Cocoa Butter During Static Crystallization, *Ibid.* 64:1663–1669 (1987).
5. Savage, C.M., and P.S. Dimick, Influence of Phospholipids During Crystallization of Hard and Soft Cocoa Butters, *Manuf. Confection.* 75:127–132 (1995).
6. Dimick, P.S., Influence of Composition on the Crystallization Behavior of Cocoa Butter, in *Proceedings of l'Alliance 7-Cedus The Crystallization of Food Product*, Paris, France, 1994.
7. Cormia, R.L., F.P. Price, and D. Turnbull, Kinetics of Crystal Nucleation in Polyethylene, *J. Chem. Phys.* 37:1333–1340 (1962).
8. Turnbull, D., Kinetics of Heterogeneous Nucleation, *Ibid.* 18:198–207 (1950).
9. Turnbull, D., Kinetics of Solidification of Supercooled Liquid Mercury Droplets, *Ibid.* 20:411–424 (1952).
10. Turnbull, D., and R.L. Cormia, Kinetics of Crystal Nucleation in Some Normal Alkane Liquids, *Ibid.* 34:820–831 (1961).
11. Turnbull, D., and J.C. Fischer, Rate of Nucleation in Condensed Systems, *Ibid.* 17:71–73 (1949).
12. Walstra, P., and C.H. van Beresteyn, Crystallisation of Milk Fat in the Emulsified State, *Neth. Milk Dairy J.* 29:35–65 (1975).
13. Skoda, W., and M. van den Tempel, Crystallization of Emulsified Triglycerides, *J. Colloid Sci.* 18:568–584 (1963).
14. Dickinson, E., and D.J. McClements, *Advances in Food Colloids*, Blackie Academic and Professional, Glasgow, 1996, pp. 145–244.
15. Hindle, S.A., M.J.W. Povey, and K.W. Smith, Kinetics of Crystallization in *n*-Hexadecane and Cocoa Butter Oil-in-Water Emulsions Accounting for Droplet-Collision Mediated Nucleation, *J. Colloid Interface Sci.* 232:370–380 (2000).
16. Povey, M.J.W., *Ultrasonic Techniques for Fluids Characterization*, Academic Press, New York, 1997, pp. 60–72.
17. Kloek, W., Mechanical Properties of Fats in Relation to Their Crystallization, Ph.D. Thesis, Wageningen University, Wageningen, The Netherlands, 1998.
18. Herhold, A.B., D. Ertas, A.J. Levine, and H.E. King Jr., Impurity Mediated Nucleation in Hexadecane-in-Water Emulsions, *Phys. Rev. E* 59:6946–6955 (1999).
19. McClements, D.J., E. Dickinson, and M.J.W. Povey, Crystallization in Hydrocarbon-in-Water Emulsions Containing a Mixture of Solid and Liquid Droplets, *Chem. Phys. Lett.* 172:449–452 (1990).
20. Dagleish, D.G., and J. Leaver, Dimensions and Possible Structures of Milk Proteins at Oil–Water Interfaces, in *Food Polymers, Gels and Colloids*, edited by E. Dickinson, Royal Society of Chemistry Press, Cambridge, 1991, pp. 113–122.
21. McClements, D.J., E. Dickinson, S.R. Dungan, J.E. Kinsella, J.G. Ma, and M.J.W. Povey, Effect of Emulsifier Type on the Crystallisation Kinetics of Oil-in-Water Emulsions Containing a Mixture of Solid and Liquid Droplets, *J. Colloid Interface Sci.* 160:293–297 (1993).
22. Dickinson, E., F. Kruizinga, M.J.W. Povey, and M. van der Molen, Crystallization in Oil-in-Water Emulsions Containing Liquid and Solid Droplets, *Colloids Surf. A* 81:273–279 (1993).
23. Smoluchowski, V.M., Mathematical Theory of the Kinetics of the Coagulation of Colloidal Particle, *Phys. Chem.* 92:129–168 (1917).
24. Farhi, G., M. Aoucher, and T. Mohammed-Brahim, Study of the Solid Phase Crystallization Behavior of Amorphous Splattered Silicon by X-Ray Diffraction and Electrical Measurement, *Sol. Energy Mater. Sol. Cells* 72:551–558 (2002).

[Received February 11, 2002; accepted June 3, 2002]